AUTHOR(S) Dillemuth, P., Lövdahl, P., Karskela, T., Ayo, A., Ponkamo, J., Liljenbäck, H., Paunonen, S., Kunnas, J., Rajander, J., Tynninen, O., Rosenholm, J. M., Roivainen, A., Laakkonen, P., Airaksinen, A. J., & Li, X.-G.

TITLE Switching the Chemoselectivity in the Preparation of [18F]FNA-N-CooP, a Free Thiol-Containing Peptide for Targeted Positron Emission Tomography Imaging of Fatty Acid Binding Protein 3

YEAR 2024

DOI 10.1021/acs.molpharmaceut.4c00546

CITATION Dillemuth, P., Lövdahl, P., Karskela, T., Ayo, A., Ponkamo, J., Liljenbäck, H., Paunonen, S., Kunnas, J., Rajander, J., Tynninen, O., Rosenholm, J. M., Roivainen, A., Laakkonen, P., Airaksinen, A. J., & Li, X.-G. (2024). Switching the Chemoselectivity in the Preparation of [18F]FNA-N-CooP, a Free Thiol-Containing Peptide for Targeted Positron Emission Tomography Imaging of Fatty Acid Binding Protein 3. Molecular Pharmaceutics, 21(8), 4147–4156. https://doi.org/10.1021/acs.molpharmaceut.4c00546

VERSION Accepted Manuscript

Switching the chemoselectivity in the preparation of [^{18}F]FNA-*N*-CooP, a free thiol-containing peptide for targeted PET imaging of fatty acid binding protein 3

Pyry Dillemuth,[a,b] Petter Lövdahl,[a,c] Tuomas Karskela,[d] Abiodun Ayo,[e] Jesse Ponkamo,[a,b] Heidi Liljenbäck,[a,f] Sami Paunonen,[a,b] Jonne Kunnas,[a,c] Johan Rajander,[a,g] Olli Tynninen,[h] Jessica M. Rosenholm,[c] Anne Roivainen,[a,f,i] Pirjo Laakkonen,[e,j,k] Anu J. Airaksinen,[a,b] Xiang-Guo Li[a,b,i,l]*

[a]Turku PET Centre, University of Turku, Turku, Finland.

[b]Department of Chemistry, University of Turku, Turku, Finland.

[c]Pharmaceutical Sciences Laboratory, Faculty of Science and Engineering, Åbo Akademi University, Turku, Finland.

[d]Turku Centre for Chemical and Molecular Analytics, Åbo Akademi University and University of Turku, Turku, Finland.

[e]Translational Cancer Medicine Research Program, Faculty of Medicine, University of Helsinki, Helsinki, Finland.

[f]Turku Center for Disease Modeling, University of Turku, Turku, Finland.

[g]Accelerator Laboratory, Åbo Akademi University, Turku, Finland.

[h]Department of Pathology, Helsinki University Hospital and University of Helsinki, Helsinki, Finland.

[i]InFLAMES Research Flagship, University of Turku, Turku, Finland.

[j]Laboratory Animal Centre, HiLIFE University of Helsinki, Helsinki, Finland.

[k]iCAN Flagship Program, University of Helsinki, Helsinki, Finland.

[l]Turku PET Centre, Turku University Hospital, Turku, Finland.

*__Corresponding Author:__ Assistant Professor Xiang-Guo Li, PhD, Turku PET Centre, University of Turku, Kiinamyllynkatu 4-8, FI-20520 Turku, Finland; Phone: +358 50 4485069; E-mail: xiali@utu.fi

Abstract

Fatty acid binding protein 3 (FABP3) is expressed both in tumor cells and in the tumor vasculature, making it a potential target for medical imaging and therapy. In this study, we aimed to radiolabel a CooP peptide with a free amino and thiol group, and evaluate the radiolabeled product [^{18}F]FNA-*N*-CooP for imaging FABP3 expression in breast cancer brain metastases by positron emission tomography. [^{18}F]FNA-*N*-CooP was prepared by highly chemoselective *N*-acylation and characterized using different chemical approaches. We validated its binding to the target using *in vitro* tissue section autoradiography and performed stability tests *in vitro* and *in vivo*. [^{18}F]FNA-*N*-CooP was successfully synthesized in 16.8% decay-corrected radiochemical yield with high radiochemical purity (98.5%). It exhibited heterogeneous binding on brain metastasis tissue sections from a patient with breast cancer, with foci of radioactivity binding corresponding to FABP3 positivity. Furthermore, the tracer binding was reduced by 55% in the presence of nonradioactive FNA-*N*-CooP a blocker, indicating specific tracer binding and that FABP3 is a viable target for [^{18}F]FNA-*N*-CooP. Favorably, the tracer did not bind to necrotic tumor tissue. However, [^{18}F]FNA-*N*-CooP displayed limited stability both *in vitro* in mouse plasma or human serum and *in vivo* in mouse, therefore further studies are needed to improve the stability [^{18}F]FNA-*N*-CooP to be used for *in vivo* applications.

Keywords

Autoradiography; brain metastasis; CooP peptide; fatty acid binding protein 3; ^{18}F-labeling; positron emission tomography

Abbreviations

ARG	Autoradiography
CooP	A peptide sequence of H-CGLSGLGVA-NH_2
FABP3	Fatty acid binding protein 3
FNA	6-Fluoronicotinic acid
HPLC	High-performance liquid chromatography
NMR	Nuclear magnetic resonance
PET	Positron emission tomography

1. Introduction

Fatty acid binding protein 3 (FABP3), also known as mammary-derived growth inhibitor (MDGI), is a small intracellular protein with important roles in suppressing cancer progression and metastasis by reducing integrin activity.[1–3] A study conducted in Finland with 1331 breast cancer patients showed that higher FABP3 expression in tumors associated with improved 10-year survival rates.[3] In a tissue microarray analysis of 1331 breast cancer tissue samples, FABP3 was expressed in 94.3% of the samples. On the other hand, its expression was linked to poor prognosis in patients with gliomas and glioblastomas.[4] FABP3 is not only expressed in tumor cells but also in tumor vasculature, which presents opportunities for dual targeting of "seed and soil" in cancer imaging and therapy.[5] In addition to its role in cancers, FABP3 expression has also been linked to α-synuclein aggregation in neurodegenerative diseases.[6] In light of the important roles of FABP3 in diseases, we have set out to develop radiopharmaceuticals for imaging FABP3 expression using positron emission tomography (PET). For targeting FABP3, a brain tumor-homing decapeptide sequence H-CGLSGLGVA-NH_2 has been identified with *in vivo* phage display techniques in the Laakkonen's lab, and the peptide is named CooP.[4] For conjugation purposes, alanine was added as a linker at the *N*-terminus of CooP in several bioimaging and drug delivery applications.[7–9] Recently, we have

prepared an alanine-linked radiotracer [^{18}F]FNA-*S*-ACooP.[10] [^{18}F]FNA denotes the radiolabeling moiety of [^{18}F]fluoronicotinic acid, which is derived from the prosthetic compound [^{18}F]fluoronicotinic acid 4-nitrophenyl ester [^{18}F]**1** (Fig. 1).[10] The activated esters of [^{18}F]FNA are favorable prosthetic compounds for radiolabeling of biomolecules, partially because they can be conveniently synthesized, for example by on-resin ^{18}F-fluorination.[10,11] The potential of [^{18}F]FNA-conjugated radiopharmaceuticals for clinical use has been showcased by Piflufolastat F-18, an imaging agent for PET imaging of prostate-specific membrane antigen (PSMA) expression in patients with prostate cancer.[12] ACooP features a free amino group and a free thiol group, which serve as potential sites for acylation reactions. Notably, in the presence of [^{18}F]FNA-4-nitrophenyl ester [^{18}F]**1**, acylation occurs exclusively on the thiol group, resulting in the formation of the *S*-acylated product [^{18}F]FNA-*S*-ACooP.[10] During the phage display peptide sequence identification process, the thiol group at the cysteine residue was left unconjugated, and cysteine deemed important for target binding.[9] Consequently, our goal was to develop a *N*-acylated radiotracer while preserving the thiol group free. In this study, we present a strategy to switch chemoselectivity of [^{18}F]**1** from *S*-acylation to *N*-acylation, as an objective to create a new tracer, [^{18}F]FNA-*N*-CooP. The target binding specificity was evaluated in metastatic brain tissue sections from a patient with metastatic breast cancer, and the *in vitro* stability of [^{18}F]FNA-*N*-CooP was evaluated in mouse plasma and human serum, and *in vivo* in mice.

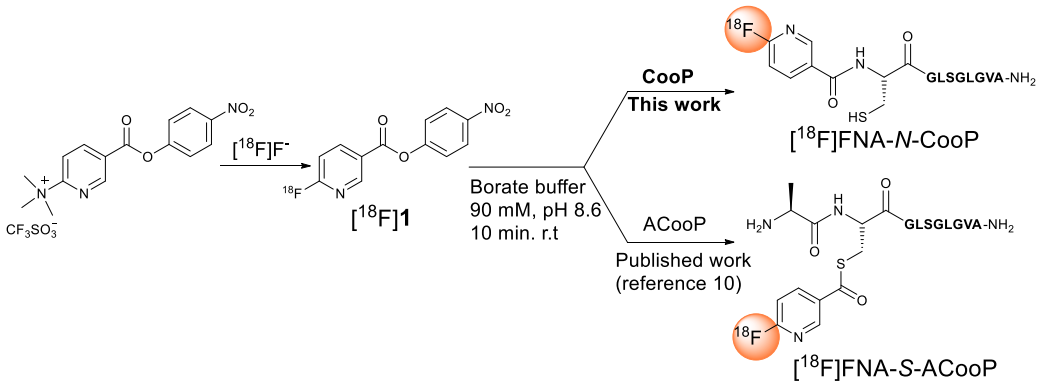

Figure 1. Chemoselective conjugation of [^{18}F]**1** with peptides CooP and ACooP.

2. Experimental section

2.1 Materials and general methods

[^{18}F]fluoride was prepared in-house at the Turku PET Centre using a cyclotron with an ^{18}O(p, n)^{18}F nuclear reaction. The precursor compound *N*,*N*,*N*-trimethyl-5-((4-nitrophenoxy)carbonyl)pyridin-2-aminium trifluoromethanesulfonate for preparing compound [^{18}F]**1** (Fig. 1) was custom-synthesized by R & S Chemicals (Kannapolis, NC, USA). The peptide CooP and FNA-*N*-CooP reference samples were custom-synthesized by United Biosystems (Herndon, VA, USA). 6-Fluoronicotinic acid (FNA) was purchased from Merck (Rahway, NJ, USA). Dako (Glostrup, Denmark) provided the monoclonal mouse anti-human PECAM/CD31 and endothelial cell antibody (clone JC70A). Secondary antibodies, including goat anti-mouse AF488 and goat anti-rabbit AF647 conjugated with Alexa Fluor (AF), were procured from Thermo Fisher (Life Technologies, Waltham, MA, USA). The Bruker Avance III 600 MHz NMR spectrometer equipped with a liquid nitrogen cooled Prodigy TCI probe and a liquid nitrogen cooled Prodigy BBO probe was employed to record NMR spectra. The chemical shifts of ^{1}H NMR were reported relative to the solvent residual proton signal of dimethyl sulfoxide (DMSO-d6: δ = 2.50 ppm), while the chemical shifts of ^{13}C NMR were reported relative to the solvent signal (DMSO-d6: δ = 39.52 ppm). The Supporting Information section provides details on the methods used for high-resolution mass spectrometry (HRMS) and liquid chromatography-mass spectrometry (LC-MS).

2.2 Radiolabeling design

The use of [^{18}F]**1** and other activated esters of [^{18}F]FNA for conjugating biomolecules has been documented in the literature.[11-14] *N*-acylation has been reported as the typical method for this purpose. However, [^{18}F]**1** can also be used for chemoselective *S*-acylation of ACooP, as we previously reported for the radiosynthesis of [^{18}F]FNA-*S*-ACooP.[10] While the reported *N*-acylation typically requires heating to accelerate the conjugation, the *S*-acylation reaction proceeded to over 95% conversion at room temperature in a commonly used biological buffer (borate buffer at pH 8.6). Interestingly, the amino group of alanine at the *N*-terminus of ACooP sequence was not reactive with [^{18}F]**1** in the presence of the adjacent thiol group as a competing nucleophile. It has been suggested that in some molecular structures, intramolecular *S*- to *N*-acyl transfer reactions may occur, leading to the formation of *N*-acylated products.[15] In the case of FNA-*S*-ACooP, acyl transfer did not occur assumedly because of an unfavorable eight-membered ring in the transition state in the acylation reaction. To enable *N*-acylation, it would be necessary to protect the thiol group of ACooP before conjugation. Instead, we sought to investigate whether removing the alanine spacer at the *N*-terminus of ACooP would facilitate intramolecular *S*- to *N*-acyl transfer, as the transition state is a five-membered ring in the case of CooP acylation. Accordingly, the CooP sequence of H-CGLSGLGVA-NH_2 was used for investigation of the radiolabeling reaction to produce [^{18}F]FNA-*N*-CooP (Fig. 1).

2.3 Preparation of FNA-*N*-CooP

The FNA-*N*-CooP compound was prepared by coupling 6-fluoronicotinic acid 4-nitrophenyl ester **1** with the CooP peptide, H-CGLSGLGVA-NH_2. The conjugation reaction was carried out by combining 33 µL of 300 mM borate buffer (pH 8.6), 100 µL of 6.5 mM CooP in H_2O (TraceSelect water, Honeywell, Charlotte, NC, USA), 33 µL of compound **1** in acetonitrile (59.3 mM), and 200 µL acetonitrile in a 1.5 mL Eppendorf tube. Upon addition of compound **1**, the reaction mixture turned bright yellow. The solution was agitated and allowed to react for 8−10 min at room

temperature. FNA-*N*-CooP was purified by semi-preparative high-performance liquid chromatography (HPLC) using a reversed phase C18 column (Jupiter Proteo, 250 × 10 mm, 4 µm, 90 Å; Phenomenex, Torrance, CA, USA). Solvent A was 0.1% formic acid in H_2O and solvent B was 0.1% formic acid in acetonitrile. The HPLC elution gradient was from 20% B to 50% B during 0–14.8 min. The product was observed at a retention time of 10.0 min, in accordance with a comparison to the commercial reference compound. The gathered fractions were dried using lyophilization, resulting in a solid product. In the present experimental setting, a small quantity of FNA-*N*-CooP was prepared at a time, which hindered the precise determination of the chemical yield.

δ^1H (600 MHz; DMSO-*d*6) 0.81 (3 H, d, Me(Val)), 0.83 (9 H, m, Me(Leu)), 0.85 (3 H, d, Me(Leu)), 0.87 (3 H, d, Me(Val)), 1.21 (3 H, d, Me(Ala)), 1.50 (4 H, m, CH_2(Leu1,2β)), 1.61 (2 H, m, CH(Leuγ)), 1.97 (1 H, m, CH(Valβ)), 2.83 (1 H, dd, CH_2(Cysβ)), 2.96 (1 H, dd, CH_2(Cysβ)), 3.57 (1 H, dd, CH_2(Serβ)), 3.61 (1 H, dd, CH_2(Serβ)), 3.72 – 3.75 (6 H, m, CH_2(Glyα)), 4.16 (1 H, dd, CH(Valα)), 4.19 (1 H, m, CH(Alaα)), 4.22 (1 H, m, CH(Serα)), 4.28 (1 H, m, CH(Leuα)), 4.39 (1 H, m, CH(Leuα)), 4.54 (1 H, m, CH(Cysα)), 5.04 (1 H, br, OH(Ser)), 6.95 (1 H, s, $CONH_2$(Ala2)), 7.18 (1 H, s, $CONH_2$(Ala2)), 7.33 (1 H, dd, 5-H(FNA)), 7.72 (1 H, d, NH(Val)), 7.90 (2 H, d, NH(Leu)), 7.98 (1 H, d, NH(Ala)), 8.06 (1 H, t, NH(Ser)), 8.07 (1 H, t, NH(Gly)), 8.21 (1 H, m, NH(Gly)), 8.44 (1 H, m, NH(Gly)), 8.45 (1 H, dt, 4-H(FNA)), 8.77 (1 H, d, 2-H(FNA)), 8.89 (1 H, d, NH(Cys)). δ^{13}C(125 MHz; DMSO-*d*6) 17.56 Me(Val), 17.92 Me(Ala), 18.80 Me(Val), 21.26 Me(Leu), 22.66 Me(Leu), 22.84 Me(Leu), 23.72 Cγ(Leu), 25.40 Cβ(Cys), 30.23 Cβ(Val), 40.52 Cβ(Leu), 41.74 Cα(Gly), 47.63 Cα(Ala), 50.45 Cα(Leu), 50.80 Cα(Leu), 55.02 Cα(Ser), 56.07 Cα(Cys), 57.13 Cα(Val), 61.27 Cβ(Ser), 109.00 (d, 5-C(FNA), 128.18 (d, 3-C(FNA), 141.53 (d, 4-C(FNA), 147.51 (d, 2-C(FNA)), 164.17 CO(FNA), 164.25 (d, 6-C(FNA)), 168.53 (CO(Gly)), 168.53 (CO(Gly)), 168.70 (CO(Gly)), 170.20 (CO(Cys)), 170.26 (CO(Val)), 170.32 (CO(Ser)), 172.09 (CO(Leu)), 172.25 (CO(Leu)), 173.98 (CO(Ala)). HRMS (ESI) m/z: $[M+H]^+$ Calculated for

$C_{38}H_{61}FN_{11}O_{11}S$ 898.4251; found 898.4257.

2.4 NMR and HRMS analysis of the commercial reference compound FNA-*N*-CooP

To establish the identity of the prepared FNA-*N*-CooP, a reference sample of FNA-*N*-CooP was acquired from United Biosystems (Herndon, VA, USA). Following the procedures described above, we performed NMR and HRMS analysis (Supporting Information) on the sample, which confirmed the identity of the synthesized peptide.

2.5 Radiosynthesis of [^{18}F]FNA-*N*-CooP

In-house produced [^{18}F]fluoride (7.0 GBq) was extracted onto a Sep-Pak Accell Plus QMA Plus Light anion-exchange cartridge (QMA; Waters, Milford, MA, USA), which was preconditioned with 0.5 M aqueous potassium carbonate (2 mL) and water (5 mL) (TraceSELECT Honeywell, Charlotte, NC, USA). Elution of [^{18}F]fluoride was carried out using a solution of Kryptofix 2.2.2 (9.2 mg, 23.1 µmol) and potassium carbonate (1.6 mg, 15.4 µmol) in Milli-Q water (76.9 µL) and acetonitrile (1.9 mL).[16] The eluate was then dried under nitrogen flow at 120 °C, followed by the addition of the precursor compound *N*,*N*,*N*-trimethyl-5-((4-nitrophenoxy)carbonyl)pyridin-2-aminium trifluoromethanesulfonate (10.0 mg, 22.2 µmol) in 0.8 mL acetonitrile. The reaction mixture was maintained at 37 °C for 10 min and then diluted with 0.1 M acetic acid (0.8 mL). [^{18}F]**1** was purified using HPLC equipped with a radioactivity detector and a reversed-phase C18 column (Jupiter Proteo, 250×10 mm, 5 µm, 90 Å; Phenomenex, Torrance, CA, USA) at a flow rate of 4 mL/min. Solvent A was 0.1% trifluoroacetic acid (TFA) in water, while solvent B was 0.1% TFA in acetonitrile. The HPLC elution gradient was from 45 to 70% B during 0–13 min. The HPLC fraction containing [^{18}F]**1** was collected and diluted with 30 mL of water, and the product was extracted onto an Oasis HLB Plus Light cartridge (Waters, Milford, MA, USA). [^{18}F]**1** was then eluted from the cartridge with acetonitrile (0.4 mL) into a solution of CooP (5.0 mg, 6.5 µmol) in borate buffer (350 µL, 300 mM, pH 8.6). The reaction mixture was kept at room temperature for 10 min and [^{18}F]FNA-*N*-CooP was purified using HPLC with a reversed-phase C18 column (Jupiter

Proteo, 250 × 10 mm, 5 μm, 90 Å; Phenomenex) at a flow rate of 4 mL/min. Solvent A was 0.1% TFA in water and solvent B was 0.1% TFA in acetonitrile. The HPLC elution gradient was 0% B during 0–5 min, and from 0% to 55% B during 5–25 min. The HPLC fraction containing [^{18}F]FNA-*N*-CooP was collected and diluted with 25 mL water containing 300 μL ascorbic acid (150 mM), and then the product was extracted onto a Sep-Pak tC18 Plus Light cartridge (Waters). [^{18}F]FNA-*N*-CooP was eluted out from the cartridge with a solution containing 250 μL ethanol, 200 μL water (TraceSELECT) and 50 μL ascorbic acid (150 mM in water) into the end product vial, which was prefilled with a solution of ascorbic acid (14 mM) in phosphate-buffered saline (PBS, 1.4 mL).

The purity and identity of the [^{18}F]FNA-*N*-CooP product were examined using HPLC. To begin the analysis, a mixture containing 0.5−0.8 MBq of [^{18}F]FNA-*N*-CooP and 10−20 nmol of cold reference FNA-*N*-CooP in water was injected into a C18 reversed-phase column (Jupiter Proteo, 250 × 4.6 mm, 5 μm, 90 Å; Phenomenex). Solvent A consisted of 0.1% TFA in water, while solvent B contained 0.1% TFA in acetonitrile. The HPLC elution gradient began at 27% B and ended at 42% B between 0−10 min, at a flow rate of 1 mL/min, and was monitored by radioactivity detection and UV detection at a wavelength of 220 nm. Samples of the final formulation (PBS with 14 mM ascorbic acid) containing [^{18}F]FNA-*N*-CooP were taken at different time points up to 4 hours and analyzed using the same analytical HPLC method. The measurement of the distribution coefficient Log$D_{7.4}$ for [^{18}F]FNA-*N*-CooP was achieved by adding 5 kBq of the tracer to a mixture of 600 μL of PBS (pH 7.4) and 600 μL of 1-octanol. The solution was thoroughly mixed using a vortexer for 3 min, followed by centrifugation for 3 min at 12,000 × g to separate the liquid layers. Aliquots of 400 μL were taken from both layers, and the radioactivity was measured using a gamma counter. The tests were performed in triplicate. The Log$D_{7.4}$ value for [^{18}F]FNA-*N*-CooP was calculated with radioactivity decay correction using the following formula: $\mathrm{Log}D = \log 10 \frac{counts\ in\ the\ octanol\ phase}{counts\ in\ the\ PBS\ phase}$.

2.6 Immunofluorescence

Eight-micrometer-thick frozen sections were fixed with 4% paraformaldehyde in PBS for 10 min,

permeabilized with 0.3% Triton X-100 in PBS, and non-specific antibody binding was blocked with a solution containing 0.03% Triton X-100 and 1% bovine serum albumin (BSA) in PBS for 1 hour at room temperature. The sections were then stained with a primary antibody against FABP3 (Mouse monoclonal IgG, sc-58275, Santa Cruz Biotechnology, Heidelberg, Germany), diluted at 1:50 in the blocking solution, and incubated overnight at 4°C, followed by a 2-hour incubation with a Alexa Fluor 488 - conjugated secondary antibody (Goat anti-mouse IgG, A-11001, Invitrogen, Thermo Fisher Scientific, Waltham, MA, USA) at room temperature. To visualize the cell nuclei, the tissue sections were counterstained with 2-(4-aminophenyl)-1H-indole-6-carboxamidine (DAPI, Vector Laboratories Inc., Newark, CA, USA) and mounted with Mowiol (Sigma-Aldrich Chemie GmbH, Steinheim, Germany) for whole digital slide scan using the Pannoramic 250 (3DHistech Ltd., H-1141 Budapest, Hungary). The images were visualized using slideviewer (3D Histech Ltd.).

2.7. TUNEL assay

Tissue sections (8 µm of thickness) were stained for necrotic and apoptotic markers using the In Situ Cell Death Detection Kit with TMR red (Roche Diagnostics GmbH, Mannheim, Germany), following the manufacturer's instructions. The sections were labeled with 50 µL of terminal deoxynucleotidyl transferase dUTP nick end labeling (TUNEL) reaction mix under dark and humidified conditions to visualize DNA strand breaks. DAPI staining was used to visualize cell nuclei.

2.8 Immunohistochemistry

Frozen sections measuring 8 micrometers in thickness were fixed with 4% paraformaldehyde in PBS for 20 min. After 10 min of incubation with 0.75% hydrogen peroxide in Milli-Q water to block endogenous peroxides, the sections were permeabilized with 0.1% Triton X-100 in 10 mM sodium citrate. To stain human blood vessels, the sections were incubated with mouse anti-human CD31 antibody (M0832, endothelial cell clone JC70A, Dako, Santa Clara, CA, USA) for 60 min, after dilution in normal antibody diluent 1:100 (Immunologic, WellMed BV, Duiven, The Netherlands),

followed by a 30-min incubation with goat anti-mouse HRP bright vision 1-step detection system (Immunologic, Duiven, The Netherlands). The staining was then visualized using the bright impact-DAB chromogenic substrate (Immunologic, Duiven, The Netherlands) after a 4-min exposure. Finally, the sections were counterstained with hematoxylin (Epredia B.V., Breda, The Netherlands) to highlight the cell nuclei, mounted and scanned with Pannoramic.

2.9 Autoradiography of [^{18}F]FNA-*N*-CooP tissue binding *in vitro*

Three slides of 20 µm-thick cryosections (three sections on each slide) of a breast cancer derived metastatic brain tissue sample from a patient were thawed at 4 °C for 15 min, and then allowed to sit at room temperature for an additional 15 min. Following this, the three slides were pre-incubated for 15 min each in three separate Falcon tubes filled with PBS (pH 7.4, 40 mL) containing FNA-*N*-CooP as a blocker at concentrations of 0 µM, 1 µM, and 10 µM, respectively. After pre-incubation, [^{18}F]FNA-*N*-CooP (16 kBq/mL) was added to each Falcon tube, and the samples were incubated for 45 min. The solutions were then discarded, and the slides were washed twice with cold PBS (4 °C) for 2 min, followed by a single dip in cold water (4 °C). The tissue sections were then dried with a light airflow and exposed to a phosphor imaging plate (BAS-TR2025, Fujifilm, Tokyo, Japan) for 18.5 hours. The study employed a phosphoimager (BAS-5000, Fujifilm, Tokyo, Japan) to scan the imaging plates. The analysis of autoradiographs was conducted using Carimas 2.10 software (Turku PET Centre, Turku, Finland, http://www.turkupetcentre.fi/carimas). The signal intensity in the tissues was expressed as photostimulated luminescence units per square millimeter (PSL/mm^2) with the background noise corrected. The same tissue sections were stained with hematoxylin-eosin (H&E) for histological analysis.

2.10 [^{18}F]FNA-*N*-CooP stability in mouse plasma and human serum *in vitro*

The stability of [^{18}F]FNA-*N*-CooP was evaluated in plasma from C57BL/6N mice. [^{18}F]FNA-*N*-CooP (0.2 MBq) was incubated in 0.3 mL of plasma at 37°C, and 50 µL samples were taken at 5 min, 10 min, and 15 min of incubation. To precipitate plasma proteins, 50 µL of acetonitrile was

added to each sample, followed by centrifugation at 14,000 × g for 1 min. The supernatant was then injected into a reverse-phase C18 column (Jupiter Proteo, 250 × 10 mm, 4 µm, 90 Å; Phenomenex) for HPLC analysis at a flow rate of 5 mL/min, with radioactivity and UV detection at a wavelength of 220 nm. The HPLC solvent A was 0.1% TFA in water, and solvent B was 0.1% TFA in acetonitrile. The elution gradient was from 15 to 55% B from 0 to 16 min. The experiments were conducted in triplicate for each time point. The presence of intact [^{18}F]FNA-*N*-CooP among the radiometabolites in the plasma samples was confirmed using a reference standard of [^{18}F]FNA-*N*-CooP. The identity of [^{18}F]FNA as one of the radiometabolites was confirmed using the corresponding non-radioactive reference FNA in the HPLC analysis. Similar experiments were performed in human serum (Supporting Information).

2.11 *In vivo* stability of [^{18}F]FNA-*N*-CooP in mice

All animal studies were approved by the national Project Authorization Board in Finland and were conducted according to the EU Directive 2010/63 on the protection of animals used for scientific purposes (license number ESAVI/3630/2023). C57BL/6N mice (male, 13-week-old, weighing 34.0 ± 1.0 g, n = 4) were obtained from the Central Animal Laboratory, University of Turku. Under anesthesia with isoflurane (4−5% for induction and 1.5−2% for maintenance), mice were administered intravenously via the tail vein with 300 µg of the enzyme inhibitor Phosphoramidon (PeptaNova GmbH, Sandhausen, Germany) in 25 µL of saline, followed immediately by an intravenous injection of [^{18}F]FNA-*N*-CooP (5.2 MBq, 53 µL) via the tail vein, or only [^{18}F]FNA-*N*-CooP without any blocking agents. One blood sample (approximately 1 mL) was taken from one mouse at one time point (5 or 15 min post-injection) using a cardiac puncture. Blood samples were collected in heparinized tubes. Blood cells and plasma were separated by centrifugation (2,100 ×g for 5 min). Plasma proteins were precipitated by adding an equal volume of acetonitrile and then pelleted by centrifugation (14,000 ×g for 2 min) at room temperature. The HPLC analysis of plasma supernatant was carried out using an instrument equipped with both a radioactivity detector and a

UV detector. The analysis was performed on a C18 column (Jupiter Proteo, 250 × 10 mm, 5 µm, 90 Å; Phenomenex) with a flow rate of 5 mL/min. Solvent A consisted of 0.1% TFA in water, while solvent B was 0.1% TFA in acetonitrile. The HPLC elution gradient began at 0% B and increased to 50% B during the first 15 min of the analysis. A mouse was first intravenously administered a mixture of enzyme inhibitors, i.e. 300 µg of Phosphoramidon and 300 µg of Lisinopril (Merck) in 50 µL of saline, followed by an injection of [^{18}F]FNA-*N*-CooP (5.6 MBq, 120 µL). The plasma supernatant was collected at 30 min post-injection and analyzed by HPLC using the same conditions as described above, apart from a slightly different elution gradient. The gradient began at 15% B and increased to 55% B during the first 16 min of the analysis, then decreased to 65% B during the final four min.

2.12 Statistical analysis

When appropriate, the results are expressed as mean values along with their standard deviation. To determine the difference between data sets, an unpaired two-tailed Student's-test with two-sample equal variance was performed. P-values less than 0.05 were considered to be statistically significant.

3. Results

3.1 Preparation and structural characterization of FNA-*N*-CooP

FNA-*N*-CooP was synthesized through a conjugation reaction between the CooP peptide and compound **1**. This reaction took place in a borate buffer within 10 min at room temperature, after which the product was purified using semi-preparative HPLC with UV detection at 220 nm. The chemical structure of FNA-*N*-CooP was determined through NMR and HRMS analyses, as shown in Supplemental Fig. S1-S5, confirming the anticipated *N*-acylated product. To determine exact chemical shifts, 1D ^{1}H- and ^{13}C-measurements were conducted along with quantification of protons (Fig. 2 and Supplemental Fig. S1). Additionally, 2D TOCSY and HSQC spectra were obtained (Supplemental Fig. S2 and S3) to provide information on the chemical shifts of both the amino acid residues and FNA moiety. HMBC spectra (Supplemental Fig. S4) provided additional information

for characterizing the molecule and determining the sequence based on the coupling of backbone amide protons with adjacent carbonyl carbons. The NMR data confirmed that FNA was attached to the amino group, not the thiol moiety. The proton spectra revealed that there were 11 nitrogen-bound protons instead of 13 or 14, depending on whether the amino group at the cysteine residue was protonated in a *S*-acylated product. In the commercial FNA-*N*-CooP reference, a thiol proton triplet was detected at 2.57 ppm and was coupled to cysteine protons in TOCSY and α- and β-carbons in HMBC. In the synthesized FNA-*N*-CooP, the thiol proton was present at the same chemical shift but displayed a broad peak and no correlation in 2D spectra. In both the synthesized and commercial FNA-*N*-CooP samples, the presence of the FNA carbonyl carbon at 164 ppm indicated the formation of an amide bond, not an expected thioester at 188 ppm. Moreover, HMBC revealed that the carbonyl carbon was connected to cysteine NH- and α-protons but not cysteine β-protons, a characteristic of a thioester product. HRMS analysis provided the anticipated results (see Supplemental Fig. S5). In the comparison analysis with the commercial reference FNA-*N*-CooP, the same set of NMR and HRMS analyses (see Supplemental Fig. S6-S11) were conducted, and the results demonstrated that our synthesized FNA-*N*-CooP was structurally identical to the commercial reference compound.

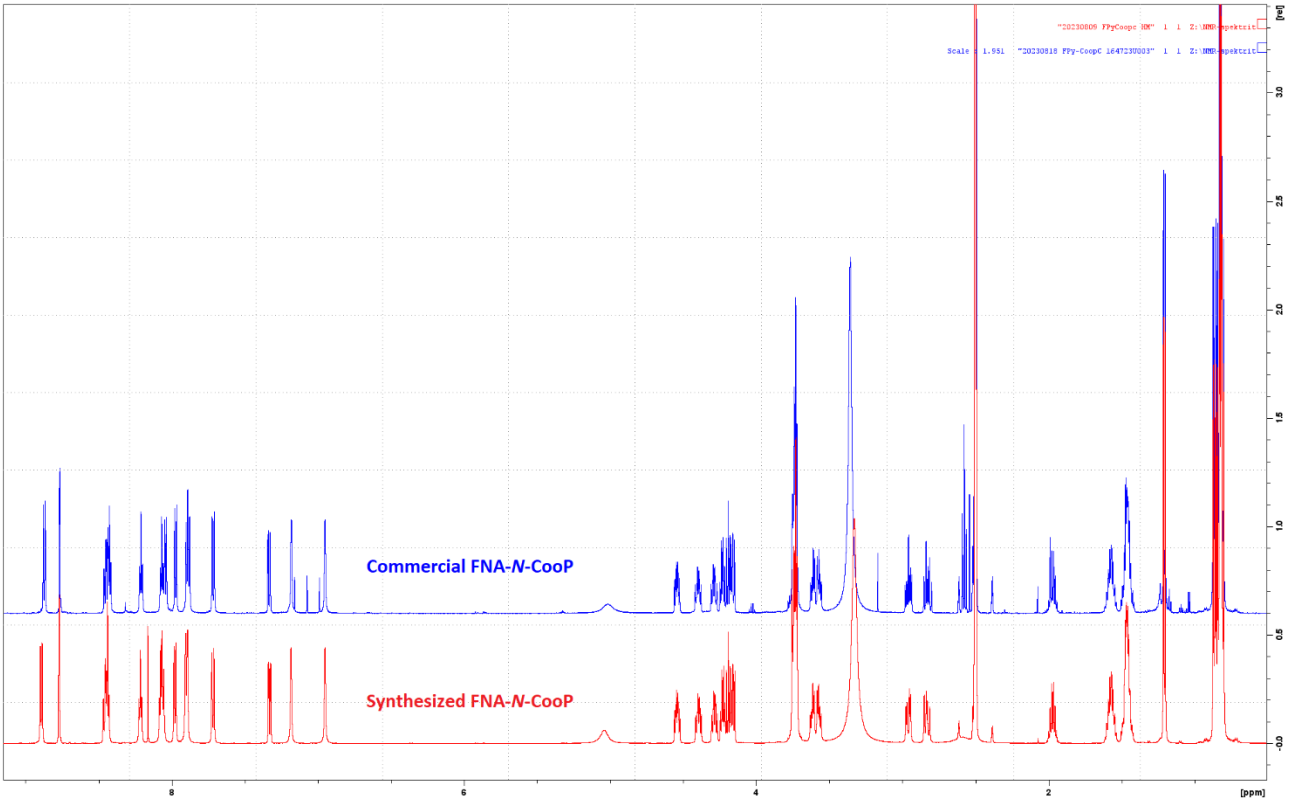

Figure 2. Comparison of ^{1}H-NMR of synthesized FNA-*N*-CooP with the commercial reference compound.

3.2 Radiochemistry of [^{18}F]FNA-*N*-CooP

In this study, we utilized a two-step synthesis process to produce [^{18}F]FNA-*N*-CooP. The first step involved the preparation of prosthetic group [^{18}F]**1**, which was synthesized using nucleophilic fluorination under mild conditions with the commonly used [K/K2.2.2]$^{+}$ ^{18}F^{-} complex. Subsequently, [^{18}F]**1** was conjugated to the CooP peptide under mild conditions to produce [^{18}F]FNA-*N*-CooP. The product was isolated using semi-preparative HPLC and formulated in PBS containing ascorbic acid. The decay-corrected radiochemical yield was 16.8% ± 5.8 (n = 3) and the radiochemical purity was 98.5% ± 0.8. The molar activity was 97.5 ± 53.2 GBq/µmol at the end of the synthesis. The total synthesis time was 171 ± 8.5 min, starting from the end of bombardment. The stability of [^{18}F]FNA-*N*-CooP in the injectable formulation (PBS with 14 mM ascorbic acid) was at least 4 h at room temperature, and long-term stability measurements deemed not necessary. The Log$D_{7.4}$ of [^{18}F]FNA-*N*-CooP was 0.30 ± 0.01 (n = 3). The chemical identity of [^{18}F]FNA-*N*-CooP was confirmed using

HPLC analysis with the reference compound FNA-*N*-CooP (Fig. 3).

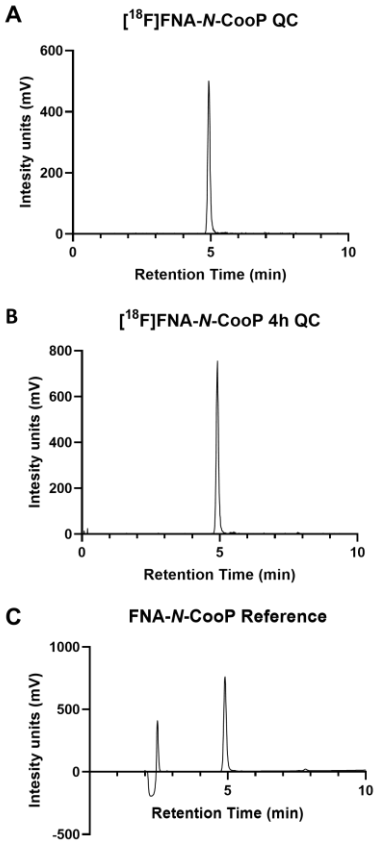

Figure 3. Quality control (QC) of [^{18}F]FNA-*N*-CooP with HPLC analysis. (A) QC at end of synthesis under radioactivity detection. (B) QC at 4 h after end of synthesis under radioactivity detection. (C) HPLC analysis of reference FNA-*N*-CooP under UV detection at wavelength of 220 nm.

3.3 *In vitro* tissue binding

In the tissue samples from the metastatic brain taken from a patient with breast cancer, a substantial amount of FABP3 expression was detected (Fig. 4A). Necrosis or apoptosis was not prominently present at this area as revealed by the TUNEL assay. Only small areas of necrosis/apoptosis were detected at the edges of some tissues. Furthermore, the presence of endothelial cells was confirmed through anti-CD31 immunohistochemistry (Fig. 4B). CD31 positivity correlated with FABP3 expression in the same tissue samples (Supplemental Fig. S12). This is consistent with the previous

observation that FABP3 expression was not limited to tumor cells but also present in tumor vasculature.[4] The subsequent tissue samples were utilized for an *in vitro* tissue binding study with [^{18}F]FNA-*N*-CooP, and heterogeneous radioactivity binding foci were observed in the areas with FABP3 expression (Fig. 4C). Binding of the radioactivity was significantly lower in the necrotic/apoptotic regions. The radioactive foci were found to correlate with tissue lesions, as indicated by H&E staining on the same tissue samples (Fig. 4D).

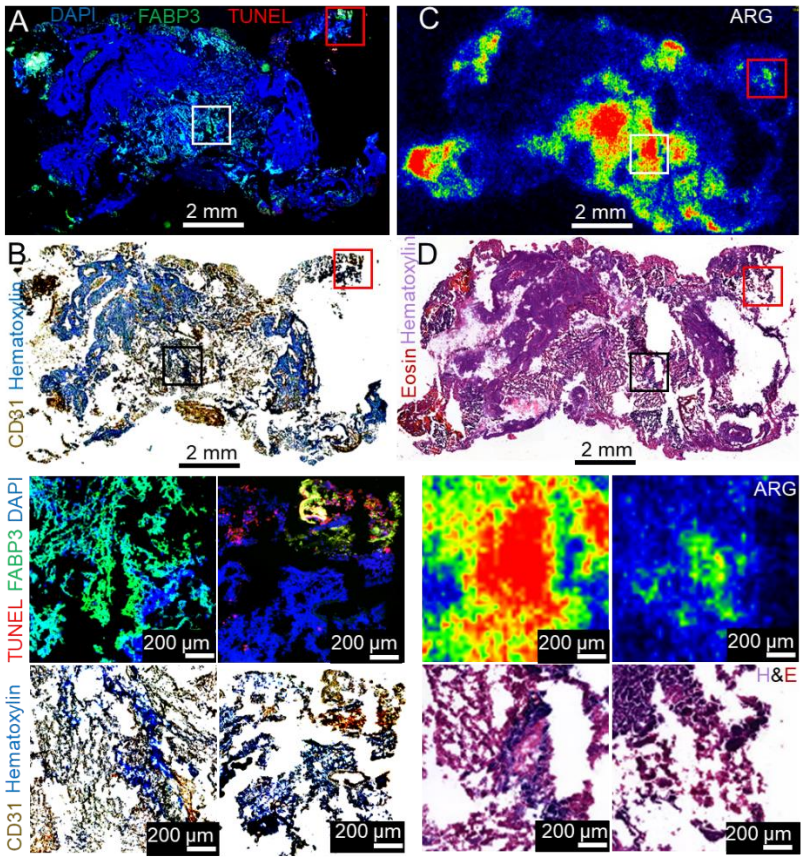

Figure 4. Correlation of tissue radioactivity binding with histology, anti-FABP3 and anti-CD31 immunostaining in human brain metastases from a patient with breast cancer. Immunofluorescence (A) and immunohistochemistry (B) of the same tissue section. Autoradiography (C) and histology (D) of the subsequent tissue section. Left panels (A) show the whole tissue sections stained for FABP3 (green), necrotic area labeled with TUNEL (red) and cell nuclei visualized with DAPI (blue). Left panel (B) show the whole tissue section stained for CD31 (brown) and cell nuclei stained for

hematoxylin (blue). Right panels (C, D) show the autoradiography and histology of the whole subsequent tissue sections. Below the left panels are magnified images of the boxed areas in A and B. Below the right panels are the magnified images of the boxed areas in C and D.

The specificity of [^{18}F]FNA-*N*-CooP's target binding was assessed by incubating tissue samples from the same patient with the compound in the presence or absence of the blocking agent, non-radioactive FNA-*N*-CooP, for 45 min at room temperature. Following rinsing and drying, the samples were imaged using autoradiography. Results showed intense, focal, and heterogeneous radioactivity binding (Fig. 5A) with a signal intensity of 84.5 ± 6.3 PSL/mm^2 (n = 3, mean of whole tissue sections). When the blocker was present at a concentration of 1 µM, the binding intensity was reduced by 37% to 53.3 ± 1.9 PSL/mm^2 (n = 3; Fig. 5B). At a concentration of 10 µM, the binding intensity was further reduced by 55% to 37.8 ± 3.7 PSL/mm^2 (n = 3; Fig. 5C). The difference in tissue binding intensity between the total-binding and blocked experiments with a 1 µM blocker was statistically significant ($P < 0.01$), as was the difference with a 10 µM blocker ($P < 0.001$) (Fig. 5 D). Furthermore, the binding intensity in the experiments with 10 µM blocker was statistically different ($P < 0.01$) from that in the experiments with a 1 µM blocker. These results indicated that the binding of [^{18}F]FNA-*N*-CooP in the tissues was specific. To correlate the radioactivity binding in the tissues with histology and FABP3 expression, the tissue sections were stained with H&E after autoradiography detection, and the subsequent 8 µm thick tissue sections were stained with anti-FABP3 antibody.

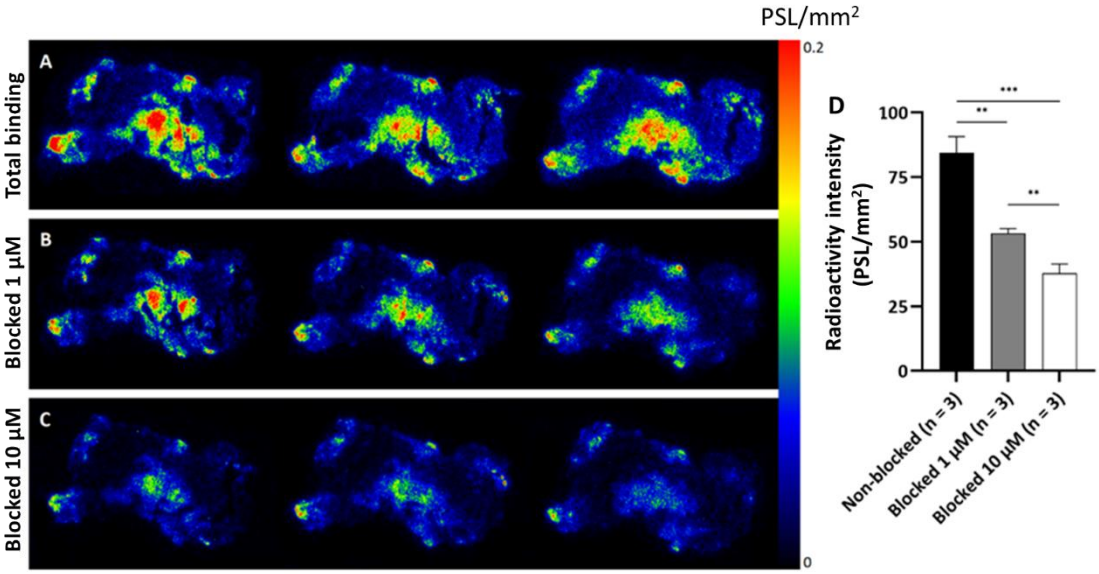

Figure 5. Autoradiography of *in vitro* binding of [^{18}F]FNA-*N*-CooP in breast cancer brain metastatic tumor tissue sections from a patient. (A) Total binding. (B) Blocking experiment with FNA-*N*-CooP at concentration of 1 µM. (C) Blocking experiment with FNA-*N*-CooP at concentration of 10 µM. (D) The differences in tissue binding intensity were statistically significant between the total binding experiments and blocking experiments (**P < 0.01 with 1 µM blocker, ***P < 0.001 with 10 µM blocker). Statistical difference (**P < 0.01) of blocking effect was also observed between the two blocking experiments with 1 and 10 µM blocker.

3.4 *In vitro* stability of [^{18}F]FNA-*N*-CooP in mouse plasma

To assess the stability of [^{18}F]FNA-*N*-CooP *in vitro*, the tracer was mixed with mouse plasma samples and incubated at 37 °C. The samples were then analyzed by HPLC at different time intervals, and a [^{18}F]FNA-*N*-CooP tracer standard was used as a reference to identify the intact tracer in the plasma samples. Additionally, FNA was used to identify [^{18}F]FNA as one of the radiometabolites. The proportion of intact tracer in the total radioactivity after 5 min, 10 min, and 15 min of incubation was 10.7% ± 0.6 (n = 3), 10.3% ± 3.5 (n = 3), and 9.1% ± 3.6 (n = 3), respectively. These results suggest that the tracer was rapidly metabolized in mouse plasma, and several radiometabolites were detected (Fig. 6C-6E). To further confirm identification of the intact tracer within the plasma

samples, tracer standard [^{18}F]FNA-*N*-CooP was added to the plasma sample at the 15-min time point, and it was observed at the anticipated retention time (12.2 min, Fig. 6F). In addition, [^{18}F]FNA was detected as one of the radiometabolites, but only in trace amounts, which indicated that the amide bond between [^{18}F]FNA and CooP peptide remained stable, suggesting that the main source of instability was the breakdown of the peptide sequence itself. In human serum, the proportion of intact tracer in the total radioactivity after 5 min and 15 min of incubation was 5.6% and 4.0%, respectively (Supplemental Fig. 13).

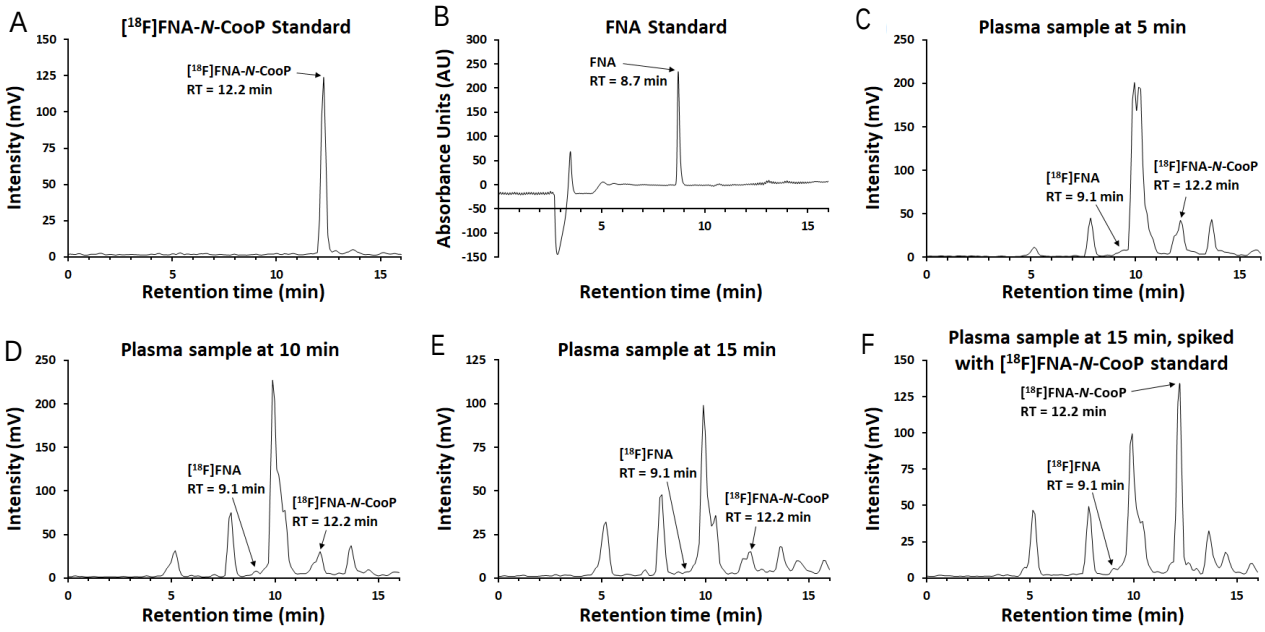

Figure 6. HPLC analysis of *in vitro* stability of [^{18}F]FNA-*N*-CooP in mouse plasma. (A) Tracer standard under radioactivity detection. (B) FNA standard under UV detection at a wavelength of 220 nm. (C−E) Plasma samples at time points of 5, 10, and 15 min under radioactivity detection. (F) Tracer standard was spiked in the plasma sample at the time point of 15 min, confirming that the peak at 12.2 min retention time was indeed intact [^{18}F]FNA-*N*-CooP.

3.5 *In vivo* stability of [^{18}F]FNA-*N*-CooP in mice

As described above, [^{18}F]FNA-*N*-CooP exhibited limited stability in mouse plasma *in vitro*. Furthermore, our results showed that [^{18}F]FNA-*N*-CooP was rapidly metabolized in healthy mice, intact tracer being 0.9% and 0.2% at 15 and 30 min post-injection, respectively. To address this issue, we tested the enzyme inhibitors Phosphoramidon and Lisinopril to improve the *in vivo* stability of [^{18}F]FNA-*N*-CooP, similar to what has been reported for other peptide tracers.[17] However, our experiments revealed that the inhibitors failed to prevent the degradation of [^{18}F]FNA-*N*-CooP *in vivo* as indicated by the HPLC analysis of the plasma samples (Supplemental Fig. S14). In the HPLC analysis, the tracer standard [^{18}F]FNA-*N*-CooP (Supplemental Fig. S14A) was used as a reference to identify the intact tracer, while FNA (Supplemental Fig. S14B) was used as a reference to identify the cleaved [^{18}F]FNA. The results showed that the amide bond was more stable than the peptide sequence itself, which was consistent with the findings from *in vitro* stability analysis in mouse plasma. The percentage of intact tracer was 5.0% and 2.3% at 5 and 15 min, respectively, in the presence of Phosphoramidon. The percentage of intact tracer was 2.1% at 30 min post-injection in the presence of both Phosphoramidon and Lisinopril. The cleaved [^{18}F]FNA percentage was 17.9% and 37.4% at 5 and 15 min, respectively, in the presence of Phosphoramidon, and 41.2% at 30 min in the presence of both Phosphoramidon and Lisinopril. To exclude the possibilities that the plasma instability was caused by the presence of Phosphoramidon, Lisinopril or heparin in the blood sampling tubes, we conducted chemical stability tests in the presence of those chemicals. The results indicated that Phosphoramidon, Lisinopril and heparin were compatible with [^{18}F]FNA-*N*-CooP (Supplemental Fig. S15).

4. Discussion

FABP3 is a clinically relevant target that has been found in cancers[1–3] and neurodegenerative diseases.[5] Our goal is to develop a radiopharmaceutical labeled with ^{18}F for PET imaging of FABP3 expression by using ACooP peptide as a targeting ligand.[10] ACooP is a peptide sequence identified through *in vivo* phage display techniques, with alanine added as a spacer to facilitate conjugation.[4]

ACooP has a free amino group and a free sulfhydryl group in its molecular structure, with the free thiol functionality considered important for target binding.[9] We planned to use the activated ester of nicotinic acid [^{18}F]**1** to conjugate ACooP by *N*-acylation at the *N*-terminus of the peptide, as reported in previous studies by others.[11–14] However, we found that in the presence of [^{18}F]**1** as the prosthetic radiolabeling agent, only the *S*-acylated product [^{18}F]FNA-*S*-ACooP was formed (Fig. 1), with a negligible amount (<3%) of the *N*-acylated product [^{18}F]FNA-*N*-ACooP observed.[10] In this work, we report the chemoselective approach for radiolabeling CooP peptide via the *N*-acylation to obtain [^{18}F]FNA-*N*-CooP.

Thioesters are typically reactive and can serve as intermediates in ligation reactions when nucleophiles like amino groups are present.[15] We suggested that the chemoselectivity could be switched by an intramolecular *S*- to *N*-acyl transfer, which could be promoted by the presence of both amino and thiol groups in close proximity. To test this hypothesis, we carried out the conjugation of the CooP sequence without the alanine spacer (section 2.3), exposing the free amino group near the free thiol group. We performed the conjugation of CooP with compound **1** in conditions simulating the radiosynthesis conditions, and then isolated the product using HPLC. The product was characterized using NMR and MS analyses, which confirmed that it was indeed the *N*-acylated compound FNA-*N*-CooP. To further confirm the identity of our in-house prepared FNA-*N*-CooP, a reference compound of FNA-*N*-CooP was custom synthesized by United Biosystems and subjected to the same sets of NMR and MS analyses. The results indicated that the two compounds were structurally identical (Fig. 2, Supplemental Fig. S1-S11). Under similar conjugation conditions as those used to prepare [^{18}F]FNA-*S*-ACooP,[10] the anticipated *N*-acylated product [^{18}F]FNA-*N*-CooP was exclusively formed, and its identity was confirmed using HPLC analysis with non-radioactive reference FNA-*N*-CooP (Fig. 3). [^{18}F]FNA-*N*-CooP remained stable in the injectable formulation for at least 4 hours.

With [^{18}F]FNA-*N*-CooP at hand, we proceeded to evaluate its target binding specificity *in vitro* using

brain metastasis tissue samples from a patient with breast cancer. We observed abundant FABP3 in these tissue samples (Fig. 4A) and visualized tumor vasculature (Fig. 4B). Necrosis was present only in small areas at the edges of the tissues. The tissues were considered suitable for evaluating FABP3 binding with [^{18}F]FNA-*N*-CooP. The tissue cryosections (n = 3) were incubated with [^{18}F]FNA-*N*-CooP in PBS for 45 min, dried, and subjected to autoradiography analysis. Intense, focal, and heterogeneous binding of radioactivity was observed in all three tissue sections (Fig. 4C and Fig. 5A). The binding foci were not in the areas of necrosis or apoptosis, which is a favorable feature from the perspective of clinical PET imaging. To confirm binding specificity, similar experiments were performed with subsequent tissue sections in the presence of FNA-*N*-CooP as a blocker at concentrations of 1 µM (Fig. 5B) and 10 µM (Fig. 5C), respectively. A statistically significant difference was observed among all the tissue binding/blocking experiments (Fig. 5D). Additionally, the radioactivity binding in the tissues was correlated with histology and FABP3 immunostaining (Fig. 4). In the previous study with [^{18}F]FNA-*S*-ACooP, the radioactivity binding to the tissue samples correlated to some extent to FABP3-positivity. However, in both cases the correlation was qualitative, and quantitative experiments would be needed for comparative studies.

The stability of [^{18}F]FNA-*N*-CooP was examined in mouse plasma through the use of HPLC quantification of intact tracer in relationship to radiometabolites. Results showed that [^{18}F]FNA-*N*-CooP had limited stability, with only 9.1% of the intact tracer remaining after 15 min of incubation in the plasma (Fig. 6). Additionally, several radiometabolites were identified. While the amide bond between the labeling moiety [^{18}F]FNA and the peptide was stable, with only a minor amount (less than 1%) of cleaved [^{18}F]FNA observed as one of the radiometabolites, the *in vivo* stability of [^{18}F]FNA-*N*-CooP was found to be lower. Despite the use of enzyme inhibitors Phosphoramidon and Lisinopril, only small proportion of intact tracer were detected in all experiments (Supplemental Fig. S 14). Previous research has shown that these enzyme inhibitors can improve the *in vivo* stability of certain radiopeptides by inhibiting specific enzymes.[17] However, in the case of [^{18}F]FNA-*N*-

CooP, the degradation mechanism may be different. Peptides are generally prone to *in vivo* degradation,[18] and the presence of a free thiol group in [^{18}F]FNA-*N*-CooP makes it more susceptible to oxidation and other modifications *in vivo*.[19] Together with our previous [^{18}F]FNA-*S*-ACooP study, we can unfortunately state that both *S*-acylated and *N*-acylated peptides showed similar instability. Possible strategies to increase the metabolic stability of [^{18}F]FNA-*N*-CooP include the use of retro-inverso analogs,[20] and engineered peptide bonds between the amino acid residues.[18]

5. Conclusion

We have successfully developed a strategy to change the chemoselectivity from *S*-acylation to *N*-acylation in the preparation of [^{18}F]FNA-*N*-CooP, a peptide with a free thiol group. [^{18}F]FNA-*N*-CooP displays focal and specific binding to brain metastatic tissue samples from a patient with breast cancer, but not in necrotic regions. [^{18}F]FNA-*N*-CooP has a suitable shelf-life for PET imaging applications, but exhibits instability *in vivo* in mice, necessitating methods for its stabilization *in vivo*. Moreover, we detected FABP3-positivity in human brain metastatic tissues, which is a new piece of evidence of high FABP3 expression in breast cancer brain metastasis. However, we acknowledge that our finding is based on a small sample size and cannot be generalized. We also demonstrate that FABP3 can be detected with [^{18}F]FNA-*N*-CooP autoradiography.

Acknowledgments

The Turku Proteomics Facility, supported by Biocenter Finland, conducted mass spectrometry analyses for our study. The Histocore unit at the University of Turku performed the H&E staining. Digitization of tissue staining was performed using a 3DHISTECH Pannoramic 250 FLASH II slide scanner at the Genome Biology Unit, which is supported by HiLIFE, the Faculty of Medicine at the University of Helsinki, and Biocenter Finland.

Funding

This research was partially supported by the Research Council of Finland's Flagship InFLAMES and the funding decision numbers were 337530 and 357910. We thank the research grants from the

Finnish Cancer Foundation, Sigrid Jusélius Foundation, the Finnish Cultural Foundation, Research Council of Finland (#350117), the Turku University Foundation, and State Research Funding of Turku University Hospital (#11009).

Declarations

Ethics approval and consent to participate

The collection of human tissue samples was approved by the ethical committee of Helsinki University Hospital, Finland. All methods were performed in accordance with the ethical standards as laid down in the Declaration of Helsinki and its later amendments or comparable ethical standards.

Consent for publication

Not applicable.

Supporting Information

This article is associated with a Supporting Information, which includes NMR and MS spectra of FNA-*N*-CooP, additional stability analysis data of [^{18}F]FNA-*N*-CooP in human serum, mice plasma, and in the presence of Phosphoramidon, Lisinopril and heparin.

Competing interests

All the authors declare that they have no competing interests.

References

(1) Amiri, M.; Yousefnia, S.; Forootan, F.S.; Peymani, M.; Ghaedi, K.; Nasr-Esfahani, M.H. Diverse roles of fatty acid binding proteins (FABPs) in development and pathogenesis of cancers. *Gene* **2018**, *676*, 171-183.

(2) Koundouros, N.; Poulogiannis, G. Reprogramming of fatty acid metabolism in cancer. *Br. J. Cancer* **2020**, *122*, 4-22.

(3) Nevo, J.; Mai, A.; Tuomi, S.; Pellinen, T.; Pentikäinen, O.T.; Heikkilä, P.; Lundin, J.; Joensuu, H.; Bono, P.; Ivaska, J. Mammary derived growth factor (MDGI) interacts with integrin α-subunits and suppresses integrin activity and invasion. *Oncogene* **2010**, *69*, 6452-6463.

(4) Hyvönen, M.; Enbäck, J.; Huhtala, T.; Lammi, J.; Sihto, H.; Weisell, J.; Joensuu, H.; Rosenthal-Aizman, K.; El-Andaloussi, S.; Langel, U.; Närvänen, A.; Bergers, G.; Laakkonen, P. Novel target for peptide-based imaging and treatment of brain tumors. *Mol. Cancer Ther*. **2014**, *13*, 996–1007.

(5) Fidler, I. The pathogenesis of cancer metastasis: the 'seed and soil' hypothesis revisited. *Nat. Rev. Cancer* **2003**, *3*, 453–458.

(6) Oizumi, H.; Yamasaki, K.; Suzuki, H.; Hasegawa, T.; Sugimura, Y.; Baba, T.; Fukunaga, K.; Takeda, A. Fatty acid binding protein 3 expression in the brain and skin in human synuleinopathies. *Front. Aging Neurosci*. **2021**, *13*, 648982.

(7) Lico, C.; Tanno, B.; Marchetti, L.; Novelli, F.; Giardullo, P.; Arcangeli, C.; Pazzaglia, S.; Podda, M. S.; Santi, L.; Bernini, R.; Baschieri, S.; Mancuso, M. Tomato bushy stunt virus nanoparticles as a platform for drug delivery to shh-dependent medulloblastoma. *Int. J. Mol. Sci*. **2021**, *22*, 10523.

(8) Feng, X.; Gao, X.; Kang, T.; Jiang, D.; Yao, J.; Jing, Y.; Song, Q.; Jiang, X.; Liang, J.; Chen, J. Mammary-derived growth inhibitor-modifed PEG-PLA nanoparticles for enhanced targeted glioblastoma therapy. *Bioconjug. Chem*. **2015**, *26*, 1850–1861.

(9) Ayo, A.; Figueras, E.; Schachtsiek, T.; Budak, M.; Sewald, N.; Laakkonen, P. Tumor-targeting peptides: the functional screen of glioblastoma homing peptides to the target protein FABP3 (MDGI). *Cancers* **2020**, *12*, 1836.

(10) Dillemuth, P.; Karskela, T.; Ayo, A.; Ponkamo, J.; Kunnas, J.; Rajander, J.; Tynninen, O.; Roivainen, A.; Laakkonen, P.; Airaksinen, A. J.; Li, X.-G. Radiosynthesis, structural identifcation and in vitro tissue binding study of [^{18}F]FNA-*S*-ACooP, a novel radiopeptide for targeted PET imaging of fatty acid binding protein 3. *EJNMMI Radiopharm. Chem.* **2024**, *9*, 16.

(11) Basuli, F.; Zhang, X.; Jagoda, E. M.; Choyke, P. L.; Swenson, R. E. Facile room temperature synthesis of fuorine-18 labeled fuoronicotinic acid-2,3,5,6-tetrafuorophenyl ester without azeotropic drying of fuorine-18. *Nucl. Med. Biol*. **2016**, *43*, 770–772.

(12) Keam, S.J. Pifufolastat F 18: diagnostic frst approval. *Mol. Diagn. Ther*. **2021**, *25*, 647–656.

(13) Zhou, Z.; McDougald, D.; Devoogdt, N.; Zalutsky, M. R.; Vaidyanathan, G. Labeling single domain antibody fragments with fuorine-18 using 2,3,5,6-tetrafluorophenyl 6-[^{18}F]fluoronicotinate resulting in high tumor to kidney ratios. *Mol Pharm.* **2019**, *16*, 214–226.

(14) Haskali, M. B.; Farnsworth, A. L.; Roselt, P. D.; Hutton, C. A. 4-Nitrophenyl activated esters are superior synthons for indirect radiofluorination of biomolecules. *RSC Med. Chem*. **2020**, *11*, 919–922.

(15) Burke, H. M.; McSweeney, L.; Scanlan, E. M. Exploring chemoselective *S*-to-*N* acyl transfer reactions in synthesis and chemical biology. *Nat. Commun.* **2017**, *24*, 15655.

(16) Li, X.-G.; Helariutta, K.; Roivainen, A.; Jalkanen, S.; Knuuti, J.; Airaksinen, A. J. Using 5-deoxy-5-[^{18}F]fluororibose to glycosylate peptides for positron emission tomography. *Nat. Protoc*. **2014**, *9*, 138-145.

(17) Nock, B. A.; Maina, T.; Krenning, E. P.; De Jong, M. "To serve and protect": enzyme inhibitors as radiopeptide escorts promote tumor targeting. *J. Nucl. Med.* **2014**, *55*, 121-127.

(18) Evans, B. J.; King, A. T.; Katsifis, A.; Matesic, L.; Jamie, J. F. Methods to enhance the metabolic stability of peptide-based PET radiopharmaceuticals. *Molecules* **2020**, *25*, 2314.

(19) Poole, L. B. The basics of thiols and cysteines in redox biology and chemistry. *Free Radic. Biol. Med*. **2015**, *80*, 148-157.

(20) Doti, N.; Mardirossian, M.; Sandomenico, A.; Ruvo, M.; Caporale, A. Recent applications of retro-inverso peptides. *Int. J. Mol. Sci*. **2021**, *22*, 8677.